Dalton Transactions

ROYAL SOCIETY OF CHEMISTRY

COMMUNICATION

View Article Online
View Journal

Cite this: DOI: 10.1039/d1dt02207e

Received 3rd July 2021,
Accepted 21st July 2021

DOI: 10.1039/d1dt02207e

rsc.li/dalton

Recomposition and storage of sunlight with intelligent phosphors for enhanced photosynthesis†

Zhijun Zhang,[a] Qinyu Han,[b] Songhan Liu,[b] Zhimin Wang,[b] Ming Hu,[b] Szeto Mun Wai Domnic,[b] Raymond Lau[c] and Bengang Xing*[b,c]

This work presents a smart solar energy regulation strategy using photon tunable long persistent phosphors as solar energy harvesting antennas to enhance overall sunlight utilization by photosynthetic organisms in multiple modes.

Photosynthesis is an essential biological process by which plants, microalgae, and other photoautotrophs capture solar energy to convert carbon dioxide, water and minerals into oxygen and energy-rich organic compounds to support all life on the Earth.[1,2] However, the crises of rapid population growth, arable land reduction and water resource scarcity have exacerbated the serious conflict between the rapidly growing demand and the inadequacy of photosynthetic products.[3] Therefore, innovations that can improve the efficiency of photosynthesis to achieve a higher output, and meanwhile, to reduce the global gap between photosynthetic production and ever-increasing consumption of photosynthetic products are in high demand.[4]

Sunlight harvesting is an initial step of photosynthesis, which supports the subsequent biological transformations and affects the overall photosynthesis efficiency.[5–7] In most plants and microalgae, solar energy harvesting mainly depends on the primary photosynthetic pigments (*e.g.* chlorophyll (*Chl*) a and b). However, due to the limited absorption band of these pigments, only less than 45% of the solar energy in the visible range from 400 to 700 nm (maximum in the blue and red regions) can be captured for photosynthesis,[8,9] while most of the solar energy in the UV and green light regions is wasted. Furthermore, the unabsorbed UV irradiation may even cause detrimental effects on the organisms and thus inhibit the photosynthesis.[10] Importantly, weather variation, which may lead to the imbalance between capturing sunlight and its full day usage, is another crucial factor that influences photosynthesis, especially during cloudy and rainy days, and at night.[11] Therefore, innovative strategies that can effectively convert the UV and green light of the solar spectrum to the photo-synthetically active blue and red light, and more significantly, can alleviate the imbalance between solar energy capture and usage for all-weather photosynthesis are exceedingly desirable.[11]

So far, several studies have been initiated through the genetic manipulation of photoluminescent materials to augment photosynthesis in diverse photoautotrophs.[12–14] For example, the photoprotection system of crops can be genetically manipulated to enable a fast response to the weather variation.[15] Likewise, the photosynthetic reaction center of microalgae can be engineered with a fluorescent protein to expand the solar energy utilization.[16,17] By taking advantage of the unique light conversion properties,[18–20] some photoluminescent materials have also been applied to broaden the spectral coverage for better matching of the absorption in photosynthetic pigments.[21–25] Although they are greatly promising to improve photosynthesis, the disadvantages including the biosafety concern, low photostability, and limited sunlight conversion remain the main technical obstacles. Moreover, none of the strategies indicates the solar energy storage capability that supports the great possibility for all-weather photosynthesis. Hence, the development of an intelligent and unique light management system that can fully use solar energy for efficient photosynthesis is still a great challenge.

Long persistent phosphors (LPPs), a particular type of phosphorescent material, are capable of storing the excitation energy from solar or room light and then emitting for minutes to hours after the excitation stoppage.[26,27] So far, these materials have received increasing research interest for a wide variety of applications in safety displays, decoration, photocatalysis, photovoltaic solar cells, bioimaging and theranostics.[28–41] Such outstanding optical properties of LPPs

[a]*Key Laboratory of Surface & Interface of Polymer Materials of Zhejiang Province, Department of Chemistry, Zhejiang Sci-Tech University, Hangzhou 310018, China*
[b]*Division of Chemistry and Biological Chemistry, School of Physical & Mathematical Sciences, Nanyang Technological University, Singapore, 637371, Singapore. E-mail: bengang@ntu.edu.sg*
[c]*School of Chemical and Biomedical Engineering, Nanyang Technological University, 62 Nanyang Drive, Singapore 637459, Singapore*

†Electronic supplementary information (ESI) available. See DOI: 10.1039/d1dt02207e

well meet the requirements for efficient and all-weather photosynthesis.

As the finest example of a solar energy converting organism in nature, microalgae possess the unique properties of fast growth, minimal water demand, and high space utilization.[42] Given the diverse valuable bioproducts such as proteins, carotenoids, or polyunsaturated fatty acids they can offer, microalgae have long been considered as highly promising sustainable resources for food supplements, animal feedstocks, and biofuels.[43,44] Therefore, by taking advantage of the photoregulation properties in LPP materials, we present an intelligent and omnidirectional solar power management strategy for enhanced photosynthesis in diverse microalgae species. With our rational design, a unique core–shell long persistent phosphor with a robust sunlight recomposition and storage capacity is developed to match the requirement of full utilization of solar radiation in photosynthesis (Scheme 1). Upon integration of such photon tunable phosphors with an ingeniously designed porous 3D scaffold, the photosynthesis efficiency of microalgae can be significantly augmented.

First, we synthesized the long persistent phosphors $Sr_{0.2}Ca_{0.8}S:Eu^{2+}@Sr_2MgSi_2O_7:Eu^{2+},Dy^{3+}$ through a two-step solid-state reaction procedure (Fig. 1 and S1†). A core–shell structure was designed to maximize the solar energy modulation of the phosphors (Fig. 1a). The core ($Sr_{0.2}Ca_{0.8}S:Eu^{2+}$) is a red emission phosphor which can convert green light to red light with a high quantum efficiency,[45] while the shell ($Sr_2MgSi_2O_7:Eu^{2+},Dy^{3+}$) is one classical phosphor that can efficiently convert UV light to blue; meanwhile, it can also store the UV light to give a bright blue afterglow emission that lasts for hours.[46] The morphology, crystalline structure, and components of the obtained phosphors were characterized by scanning electron microscopy (SEM), X-ray diffraction (XRD), and energy dispersive X-ray spectroscopy (EDS), respectively. Apparently, such phosphors showed an irregular morphology with good dispersibility (Fig. S2†). The characteristic diffraction peaks in the XRD patterns evidently demonstrated the well-crystallized structure of $Sr_{0.2}Ca_{0.8}S$ and $Sr_2MgSi_2O_7$ (Fig. S3†). Meanwhile, the EDS maps revealed the uniform element distribution and the successful doping with Eu and Dy (Fig. S4†). The confocal microscopy images strongly suggest the core–shell structure of the phosphors, in which the red luminescent cores were uniformly encapsulated with the blue luminescent shells (Fig. 1b–d and S5†). All these results clearly indicate the successful synthesis of the unique phosphors.

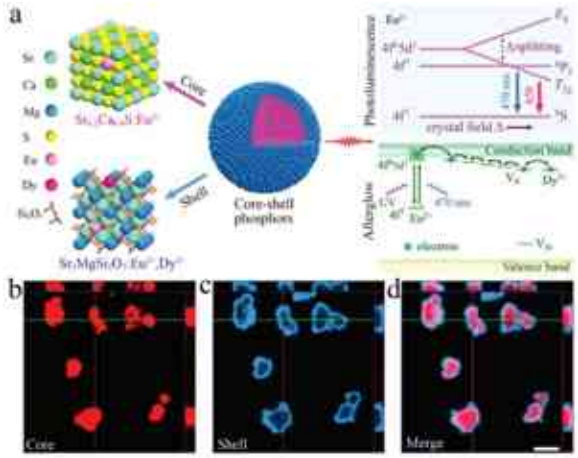

Fig. 1 (a) The structure and luminescence mechanisms of the core–shell long persistent phosphors. Confocal microscopy images (Z-stack projection) of the phosphors: (b) red channel (E_x: 560 nm, E_m: 600–700 nm), (c) blue channel (E_x: 405 nm, E_m: 430–500 nm), and (d) the merged. Scale bar = 10 μm.

Next, we investigated the photoluminescence behavior of the phosphors to confirm their solar energy conversion ability (Fig. 2). The emission spectra upon excitation at 365 nm (UV light) and 530 nm (green light) were first obtained. As shown in Fig. 2a, upon 365 nm excitation, two emission peaks at 470 nm and 650 nm were observed, which fall in the blue and red regions of the CIE 1931 chromaticity diagram with the

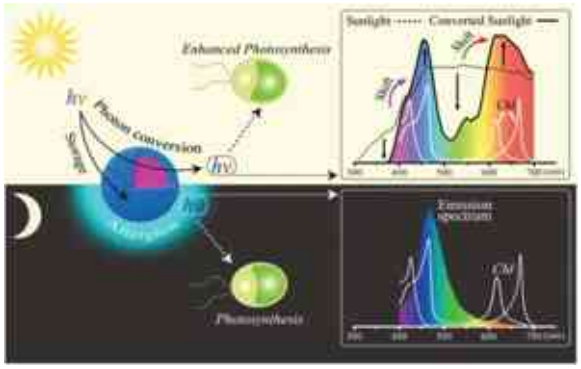

Scheme 1 Schematic illustration of the solar energy conversion and storage by the phosphors for the enhanced and potential all-weather photosynthesis.

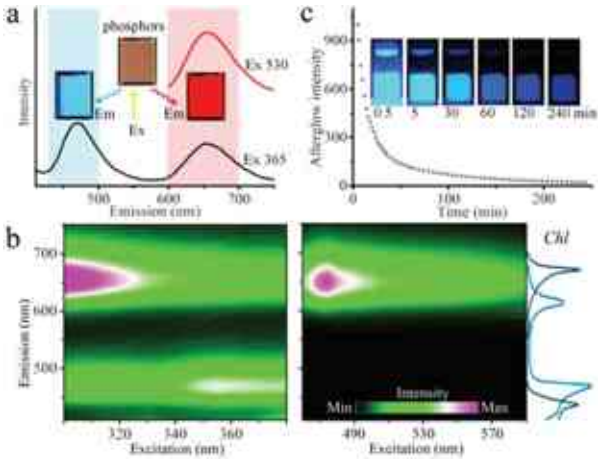

Fig. 2 (a) The images and emission spectra of the phosphors, (b) the excitation–emission maps of the phosphors under the excitation in the UV (left) and green (right) light regions, and the curves on the right side are the absorption spectra of chlorophyll a and b, and (c) the afterglow images and decay curves.

color coordinates of (0.1799; 0.2014) and (0.7078; 0.2921), respectively (Fig. S6†). Meanwhile, upon 530 nm excitation, a red emission peak with the same shape as that on excitation at 365 nm appeared. Such emissions could be ascribed to the $4f^6 5d^1 \rightarrow 4f^7$ transition of Eu^{2+} in the core and shell structure, respectively (Fig. 1).[21,26] The light conversion of the phosphors in the broad UV (*e.g.* 300–380 nm) and green (*e.g.* 480–590 nm) spectral regions was then confirmed from the excitation–emission matrix, in which the strong emission bands that well overlapped with the absorption bands of the photosynthesis pigments were observed (Fig. 2b). Furthermore, as shown in Fig. 2c, after the stoppage of UV light irradiation, a bright blue afterglow emission that could last for more than 4 hours was also observed. This long-lasting luminescence could be attributed to the storage and retention of the photo-excited electrons from the $4f^7 \rightarrow 4f^6 5d^1$ transition of Eu^{2+} by the conduction band of $Sr_2MgSi_2O_7$ (Fig. 1a).[26] The spectrum of the afterglow emission greatly overlapped with the absorption spectra of the photosynthetic pigments (Fig. S7†). These optical characteristics clearly indicated that the obtained phosphors are very promising for efficiently converting the photosynthetically harmful UV region and the low active green region of the sunlight into photo-synthetically active blue and red light that can be fully utilized by photosynthetic organisms in nature. Importantly, such phosphors are highly capable of storing solar energy to emit under gloomy and dark conditions, which could thus serve as a highly efficient photosynthesis platform working under all-weather conditions. Notably, beside the advanced solar energy regulation capability, the core–shell phosphors' structure also showed a promising stability for their application in aqueous solution (Fig. S8†).

In order to fully utilize the sunlight-regulating function of the phosphor materials in photosynthetic organisms, we further fabricated a phosphor doped porous 3D scaffold (**PP3DS**) as the culture platform. Typically, **PP3DS** was prepared through a sacrificial template method with polystyrene (PS) sponge as the template and a phosphor doped agarose hydrogel as the skeletal material (Fig. 3a). The resulting scaffold showed a highly porous structure composed of a well-interconnected spherical pore network with an average pore size of more than 200 μm and a porosity of up to 70% (Fig. 3b and S9†), which is sufficient to provide enough space for microalgae (~10 μm in diameter) cultivation. Growing in a cavity surrounded by the matrix encapsulated with phosphors, microalgae can, to the utmost extent, utilize the converted light and afterglow emission. Moreover, this porous cultivation system can greatly facilitate light dilution and prove uniform distribution to further improve the overall sunlight utilization by photosynthetic organisms.

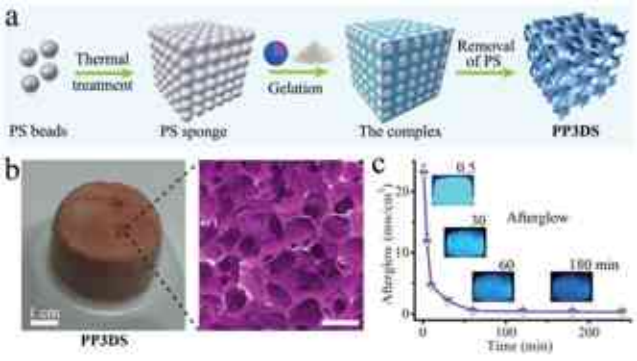

Fig. 3 (a) Fabrication of **PP3DS**. (b) Photographs of **PP3DS** and its morphology (scale bar = 500 μm). (c) The time-lapse images and afterglow intensity of **PP3DS** after 30 min solar irradiation.

The afterglow light density of the scaffold was also measured to explore the possibility of the afterglow emission to initiate photosynthesis. Typically, after 30 min sunlight irradiation, the scaffold can give a strong afterglow emission over 4 mW cm^{-2} in the first 30 min. Even after 4 h, the afterglow intensity is higher than 0.3 mW cm^{-2}, although this value is much lower than the sunlight intensity, which is enough to trigger photosynthesis in microalgae.[47] Considering the microalgal growth within the scaffold cavities, which is surrounded by and also close to the afterglow of the phosphors, the actual light harvested by microalgae will be likely much higher than the measured value. Furthermore, such **PP3DS** exhibited promising stability. There was no apparent attenuation in the optical properties of the scaffold even after one-month placement (Fig. S10†). Meanwhile, there were no obvious metal elements dissolved in water after immersion with PP3DS (Fig. S11†), clearly indicating its stability for long-term usage with minimal concern for environmental contamination.

We then investigated the growth of microalgae using **PP3DS** as the culture scaffold. The indoor culture under a metal-halide lamp, a commonly used light source to mimic the sunlight, was first shown with one typical model microalga, *Chlorella vulgaris* (*C. vulgaris*). As a frequently studied green unicellular microalga, *C. vulgaris* is also known as an important source of dietary supplements containing a high level of proteins, vitamins, and unsaturated fatty acids.[48] In order to simulate the weather variation, the cultivation was exposed to 9 h of daily light irradiation with a light/dark cycle of 1.5 h/0.5 h applied. After cultivation under different conditions, the microalgae were harvested and the density was quantified by monitoring the absorbance at 680 nm (OD_{680}). Notably, compared with plant microalgae that have a very short growth cycle of just a few days, in our experiment, the OD_{680} value of microalgae was used to monitor the cultivation. As shown in Fig. 4a, after a four-day cultivation in the pure culture medium, the optical density of microalgae increased by about 0.3. As expected, the increment greatly enhanced when **PP3DS** was immersed in the medium as the culture scaffold (Fig. 4a). Moreover, this enhancement increases gradually with the increasing amount of phosphors doped in **PP3DS** and tends to be stable when the doping amount reaches 60 mg mL^{-1}. At the doping amount of 60 mg mL^{-1}, the increment of the microalgae density (OD_{680}) in **PP3DS** reaches 0.7, which is ~1.3 fold higher than that in the pure medium. Using **PP3DS** as the culture carrier, significantly enhanced photosynthesis was also

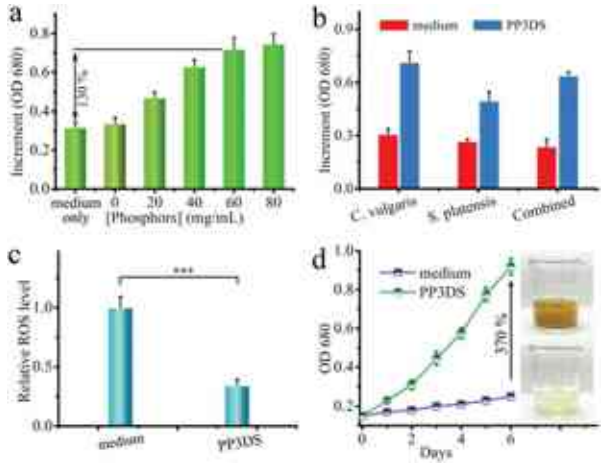

Fig. 4 (a) Growth of *C. vulgaris* in medium and in the presence of **PP3DS** fabricated with different phosphor concentrations. (b) The growth of different microalgae species in medium with or without **PP3DS.** (c) The relative ROS levels in *C. vulgaris* cultured with or without PP3DS. Significant difference: ***$P < 0.001$. (d) The outdoor growth curves of *C. vulgaris* with or without **PP3DS.**

achieved in other different industrial microalgae species (Fig. 4b), revealing the versatility of our energy converting and storing system for efficient photosynthetic applications in different organisms.

To understand the intrinsic roles of light regulation in enhancing photosynthesis, we studied the growth of microalgae under different light irradiation. As shown in Fig. S12,† neither the continuous UV light nor the green light alone could support the fast growth in microalgae. However, under the same UV and green light conditions, a significant enhancement in the microalgae growth was readily achieved in our **PP3DS** culture system, strongly suggesting the capability of **PP3DS** to transfer photosynthetically harmful UV and low active green light to photosynthetically active radiation that augments the photosynthesis efficiency. Moreover, on cultivation under dark conditions, no apparent growth of microalgae was found, while in the presence of irradiated PP3DS, obvious growth of microalgae was observed (Fig. S13†). These results clearly suggest the possibility of the afterglow effect to support photosynthesis during dark conditions. Additionally, the photon conversion would eliminate the harmful UV light, which could be another reason for the enhanced photosynthesis.[10] Indeed, compared with that placed under dark conditions, microalgae cultured in the medium under light irradiation without **PP3DS** exhibited obvious ROS stress (Fig. 4c and S14†). Notably, a remarkable ROS decrease was observed on using **PP3DS** as the culture carrier (Fig. 4c and S14†). These results suggested that **PP3DS** can shift UV light irradiation and thus minimize the adverse effect on photosynthesis caused by ultraviolet light.

Considering the feasibility of the **PP3DS** scaffold in industrial bio-production, we validated its performance in outdoor culture under direct solar irradiation. As shown in Fig. 4d, the microalgae showed a very low growth rate even after six days of cultivation in the medium without **PP3DS.** Excitingly, in the presence of **PP3DS**, a 3.7-fold increase in the photosynthetic output could be easily achieved with the net production increased by more than 5-fold. Moreover, this **PP3DS** scaffold can be reused for different cycles without noticeable attenuation in the performance (Fig. S15†), thus unequivocally indicating the promising capability of the as-developed scaffold towards outdoor cultivation.

In summary, we have demonstrated a smart photosynthesis platform with a robust sunlight recomposition and storage capability that could significantly augment the photosynthesis efficiency in different photosynthetic models. Using this platform the photosynthesis in microalgae was significantly enhanced by more than 1-fold in indoor culture and more than 5-fold in outdoor culture under direct solar irradiation. Moreover, this platform is environment-friendly, stable, and reusable, which provides valuable solutions towards augmented photosynthesis, and would thus boost the economic viability of microalgal food or biofuel industrial production in the near future. It is true that there is still a long way to go to industrialize the current system. To realize the industrial application of the current system several research studies from the following aspects should be further performed, including (i) simplifying the synthesis process of phosphor materials for mass synthesis, (ii) using glass or other materials to construct phosphor doped porous 3D scaffolds to further improve the stability and long-term usability, and (iii) construction of reaction vessels with gas supplement function and microalgae harvest assist function for large-scale cultivation.

Conflicts of interest

There are no conflicts to declare.

Acknowledgements

Z.Z. acknowledges the financial support from the National Natural Science Foundation of China (NSFC) (No. 22007083), the Zhejiang Provincial Natural Science Foundation of China (Grant No. LQ20B010010), and the Science Foundation of Zhejiang Sci-Tech University (ZSTU) under Grant No. 19062410-Y. B.X. acknowledges the financial support from Tier 1 RG6/20, 04MNP002205C230, A*Star 002425-00001, SERC A1983c0028 and the National Natural Science Foundation of China (NSFC) (No. 51929201).

References

1 E. Romero, V. I. Novoderezhkin and R. van Grondelle, *Nature*, 2017, **543**, 355–365.
2 H. Zhang, H. Liu, Z. Tian, D. Lu, Y. Yu, S. Cestellos-Blanco, K. K. Sakimoto and P. Yang, *Nat. Nanotechnol.*, 2018, **13**, 900–905.

3 J. M. Jez, S. G. Lee and A. M. Sherp, *Science*, 2016, **353**, 1241–1244.
4 S. P. Long, A. Marshall-Colon and X.-G. Zhu, *Cell*, 2015, **161**, 56–66.
5 K. Amarnath, D. I. G. Bennett, A. R. Schneider and G. R. Fleming, *Proc. Natl. Acad. Sci. U. S. A.*, 2016, **113**, 1156–1161.
6 D. G. Nocera, *Acc. Chem. Res.*, 2017, **50**, 616–619.
7 G. Longatte, A. Sayegh, J. Delacotte, F. Rappaport, F.-A. Wollman, M. Guille-Collignon and F. Lemaître, *Chem. Sci.*, 2018, **9**, 8271–8281.
8 M. Chen and R. E. Blankenship, *Trends Plant Sci.*, 2011, **16**, 427–431.
9 R. E. Blankenship and M. Chen, *Curr. Opin. Chem. Biol.*, 2013, **17**, 457–461.
10 P. J. Neale, R. F. Davis and J. J. Cullen, *Nature*, 1998, **392**, 585.
11 M. D. Ooms, C. T. Dinh, E. H. Sargent and D. Sinton, *Nat. Commun.*, 2016, **7**, 12699.
12 R. Croce and H. van Amerongen, *Nat. Chem. Biol.*, 2014, **10**, 492–501.
13 L. Wondraczek, E. Tyystjärvi, J. Méndez-Ramos, F. A. Müller and Q. Zhang, *Adv. Sci.*, 2015, **2**, 1500218.
14 S. Hong, M. Song, S. Kim, D. Bang, T. Kang, I. Choi and L. P. Lee, *ACS Nano*, 2016, **10**, 5635–5642.
15 J. Kromdijk, K. Głowacka, L. Leonelli, S. T. Gabilly, M. Iwai, K. K. Niyogi and S. P. Long, *Science*, 2016, **354**, 857–861.
16 W. Fu, A. Chaiboonchoe, B. Khraiwesh, M. Sultana, A. Jaiswal, K. Jijakli, D. R. Nelson, A. a. Al-Hrout, B. Baig, A. Amin and K. Salehi-Ashtiani, *Sci. Adv.*, 2017, **3**, e1603096.
17 K. J. Grayson, K. M. Faries, X. Huang, P. Qian, P. Dilbeck, E. C. Martin, A. Hitchcock, C. Vasilev, J. M. Yuen, D. M. Niedzwiedzki, G. J. Leggett, D. Holten, C. Kirmaier and C. Neil Hunter, *Nat. Commun.*, 2017, **8**, 13972.
18 F. Pu, L. Wu, X. Ran, J. Ren and X. Qu, *Angew. Chem., Int. Ed.*, 2014, **54**, 892–896.
19 G. Li, Y. Zhao, Y. Wei, Y. Tian, Z. Quan and J. Lin, *Chem. Commun.*, 2016, **52**, 3376–3379.
20 Z. Xia and A. Meijerink, *Chem. Soc. Rev.*, 2017, **46**, 275–299.
21 L. Wondraczek, M. Batentschuk, M. A. Schmidt, R. Borchardt, S. Scheiner, B. Seemann, P. Schweizer and C. J. Brabec, *Nat. Commun.*, 2013, **4**, 2047.
22 J. P. Giraldo, M. P. Landry, S. M. Faltermeier, T. P. McNicholas, N. M. Iverson, A. A. Boghossian, N. F. Reuel, A. J. Hilmer, F. Sen, J. A. Brew and M. S. Strano, *Nat. Mater.*, 2014, **13**, 400–408.
23 Y. Wang, S. Li, L. Liu, F. Lv and S. Wang, *Angew. Chem., Int. Ed.*, 2017, **56**, 5308–5311.
24 Y. Xu, J. Fei, G. Li, T. Yuan, X. Xu, C. Wang and J. Li, *Angew. Chem., Int. Ed.*, 2018, **57**, 6532–6535.
25 W.-T. Huang, T.-Y. Su, M.-H. Chan, J.-Y. Tsai, Y.-Y. Do, P.-L. Huang, M. Hsiao and R.-S. Liu, *Angew. Chem., Int. Ed.*, 2021, **60**, 6955–6959.
26 Y. Li, M. Gecevicius and J. Qiu, *Chem. Soc. Rev.*, 2016, **45**, 2090–2136.
27 J. Xu, J. Zhou, Y. Chen, P. Yang and J. Lin, *Coord. Chem. Rev.*, 2020, **415**, 213328.
28 W. Fan, N. Lu, C. Xu, Y. Liu, J. Lin, S. Wang, Z. Shen, Z. Yang, J. Qu, T. Wang, S. Chen, P. Huang and X. Chen, *ACS Nano*, 2017, **11**, 5864–5872.
29 Z. Pan, Y.-Y. Lu and F. Liu, *Nat. Mater.*, 2012, **11**, 58–63.
30 J. Wang, Q. Ma, W. Zheng, H. Liu, C. Yin, F. Wang, X. Chen, Q. Yuan and W. Tan, *ACS Nano*, 2017, **11**, 8185–8191.
31 Q. Miao, C. Xie, X. Zhen, Y. Lyu, H. Duan, X. Liu, J. V. Jokerst and K. Pu, *Nat. Biotechnol.*, 2017, **35**, 1102–1110.
32 Y. Su, S. Z. F. Phua, Y. Li, X. Zhou, D. Jana, G. Liu, W. Q. Lim, W. K. Ong, C. Yang and Y. Zhao, *Sci. Adv.*, 2018, **4**, eaas9732.
33 Z. Li, Y. Zhang, X. Wu, L. Huang, D. Li, W. Fan and G. Han, *J. Am. Chem. Soc.*, 2015, **137**, 5304–5307.
34 Z. Li, Y. Zhang, X. Wu, X. Wu, R. Maudgal, H. Zhang and G. Han, *Adv. Sci.*, 2015, **2**, 1500001.
35 Z. Zhou, W. Zheng, J. Kong, Y. Liu, P. Huang, S. Zhou, Z. Chen, J. Shi and X. Chen, *Nanoscale*, 2017, **9**, 6846–6853.
36 J. Duan, J. Wang, Q. Tang, B. He and W. Wang, *Chem. Commun.*, 2017, **53**, 3209–3212.
37 M. Zhao, Q. Zhang and Z. Xia, *Acc. Mater. Res.*, 2020, **1**, 137–145.
38 J. Song, X. Chen and H. Yang, *Chem. Soc. Rev.*, 2019, **48**, 3073–3101.
39 G. Cui, X. Yang, Y. Zhang, Y. Fan, P. Chen, H. Cui, Y. Liu, X. Shi, Q. Shang and B. Tang, *Angew. Chem., Int. Ed.*, 2019, **131**, 1354–1358.
40 H.-F. Wang, X. Chen, F. Feng, X. Ji and Y. Zhang, *Chem. Sci.*, 2018, **9**, 8923–8929.
41 S. Yang, D. Wu, W. Gong, Q. Huang, H. Zhen, Q. Ling and Z. Lin, *Chem. Sci.*, 2018, **9**, 8975–8981.
42 J. Ruiz, G. Olivieri, J. de Vree, R. Bosma, P. Willems, J. H. Reith, M. H. M. Eppink, D. M. M. Kleinegris, R. H. Wijffels and M. J. Barbosa, *Energy Environ. Sci.*, 2016, **9**, 3036–3043.
43 J. L. García, M. de Vicente and B. Galán, *Microbiol. Biotechnol.*, 2017, **10**, 1017–1024.
44 R. H. Wijffels and M. J. Barbosa, *Science*, 2010, **329**, 796–799.
45 X. Qin, X. Liu, W. Huang, M. Bettinelli and X. Liu, *Chem. Rev.*, 2017, **117**, 4488–4527.
46 Y. Lin, Z. Tang, Z. Zhang, X. Wang and J. Zhang, *J. Mater. Sci. Lett.*, 2001, **20**, 1505–1506.
47 S. P. Singh and P. Singh, *Renewable Sustainable Energy Rev.*, 2015, **50**, 431–444.
48 Y. Panahi, B. Darvishi, N. Jowzi, F. Beiraghdar and A. Sahebkar, *Curr. Pharm. Des.*, 2016, **22**, 164–173.